RevMexAA (Serie de Conferencias), **30**, 49–56 (2007)

SUPERNOVA EXPLOSIONS IN WINDS AND BUBBLES, WITH APPLICATIONS TO SN 1987A

Vikram V. Dwarkadas[1]

RESUMEN

Las estrellas masivas pueden modificar significativamente el medio que las rodea durante sus vidas. Cuando las estrellas explotan como supernovas, la onda de choque resultante se expande dentro de este medio modificado y no en el medio interestelar. Exploramos la evolución del medio alrededor de las estrellas masivas, y la expansión de la onda de choque dentro de este medio. Entonces aplicamos estos resultados para comprender la expansión de la onda de choque en el medio ambiente que rodea a SN 1987A, y la evolución de la emisión en radio y rayos X en este caso.

ABSTRACT

Massive stars can significantly modify the surrounding medium during their lifetime. When the stars explode as supernovae, the resulting shock wave expands within this modified medium and not within the interstellar medium. We explore the evolution of the medium around massive stars, and the expansion of the shock wave within this medium. We then apply these results to understanding the expansion of the shock wave in the ambient medium surrounding SN 1987A, and the evolution of the radio and X-ray emission in this case.

Key Words: **CIRCUMSTELLAR MATTER — HYDRODYNAMICS — SHOCK WAVES — SUPERNOVAE: GENERAL — SUPERNOVAE: INDIVIDUAL (SN 1987A)**

1. INTRODUCTION

Core-collapse supernovae (SNe) arise from massive stars ($\gtrsim 8M_{\odot}$). These stars tend to modify the medium around them substantially, often leading to the formation of circumstellar (CS) wind-blown bubbles around the star. At the end of its life when the star explodes as a SN, the resulting shock wave will interact with the modified environment before it reaches the interstellar medium (ISM) which in some cases may take a substantially long time. The subsequent evolution of the shock wave, and the radiation signatures from the supernova remnant (SNR) will depend crucially on the structure and dynamics of the surrounding medium. In this paper we examine the structure of the CS environment around stars, and the aftermath of stellar explosions which occur within this environment. Finally we apply the lessons learned to one of the most fascinating and well-studied objects, SN 1987A. In § 2 we study the formation of the ambient medium around massive stars. In § 3 we discuss the evolution of SNe in this medium. Finally in § 4 we focus on applying these results to understanding the evolution and radiation signatures from SN 1987A.

[1]Dept. of Astronomy and Astrophysics, Univ. of Chicago, 5640 S Ellis Ave., AAC 010c, Chicago, IL 60637, USA (vikram@oddjob.uchicago.edu).

2. THE ENVIRONMENTS OF MASSIVE STARS

The environment of a massive star depends on its zero-age main-sequence mass, its rotational velocity, the metallicity, and the presence of other nearby stars, among other factors. Therefore the evolution can be quite complicated, but several common factors exist. There has been significant discussion of the evolution of massive stars by Norbert Langer at this conference, and a highly comprehensive review of observations of the circumstellar medium (CSM) around massive stars was given by You-Hua Chu. Therefore I will concentrate here on those details that are essential to understanding the evolution of the subsequent SN shock wave upon the explosion of the star.

2.1. *Main-Sequence Stars*

Massive stars generally start their lives as main-sequence O/B stars. A star of solar metallicity during its lifetime will usually lose mass through a radiatively driven wind (Kudritzki & Puls 2000) with a mass-loss rate on order 10^{-8} to $10^{-6}M_{\odot}$ yr^{-1}, and with a wind velocity on order a few thousand km s^{-1}. The interaction of the wind from the star with the surrounding medium will lead to the formation of an interstellar wind-blown bubble (WBB), the structure of which was first delineated by Weaver et al. (1977, hereafter W77). If the wind parameters are fixed,

the bubble shows essentially 4 different regions as we go outwards in radius (1) Freely expanding wind. For a given mass-loss rate $\dot{M}$ and wind velocity v_w the density of the wind goes as $\rho_w = \dot{M}/(4\pi r^2 v_w)$. (2) A low-density, high-pressure (and therefore high temperature) region of shocked stellar wind. (3) A region of shocked ambient medium. The shocked ambient medium usually cools quickly, resulting in the formation of a thin, dense shell. (4) The unshocked ambient medium. Most of the volume is usually occupied by the region of shocked stellar wind, forming a hot, low-density cavity. W77 found a self-similar solution for the bubble with constant wind parameters, with radius varying with time as $R \propto t^{3/5}$.

Several factors may complicate this simplistic description. The wind properties are not constant but change with time as the star evolves through different phases. Hydrodynamic instabilities and the onset of turbulence may cause a change in the dynamical properties. Mixing at the interface between the hot shocked wind and the dense, cool, shocked ambient medium, which may also be a conductive interface, tends to lower the temperature in the interior. Density inhomogeneities or an asymmetric wind may lead to bubbles that are not spherical.

The radius of the outer shock of the bubble (the outer edge of the dense shell) is (Weaver et al. 1977):

$$R_{sh} = 0.76 \left(\frac{L}{\rho}\right)^{1/5} t^{3/5} \quad (1)$$

where $L = 0.5\dot{M}v_w^2$ is the mechanical luminosity of the wind, $\dot{M}$ is the wind mass-loss rate and v_w is the wind velocity. In the case of a main-sequence (MS) star with $\dot{M} = 10^{-7} M_\odot$ yr^{-1}, and velocity 2500 km s^{-1}, L is about 1.984×10^{35} ergs s^{-1}. If this lasts for about 10 million years, the total energy released will be about

$$E_{MS} = 6.25 \times 10^{49}\ \dot{M}_{-7}\ v_{2500}^2\ t_{10} \quad \text{ergs} \quad (2)$$

where $\dot{M}_{-7}$ is the mass-loss rate in terms of $10^{-7} M_\odot$ yr^{-1}, v_{2500} is the wind velocity in units of 2500 km s^{-1} and time is in units of 1 million years years ($t_{10} = 10 \times 10^6$ years).

We assume that the main sequence star is formed in a medium with an average density of about 2.34×10^{-23} g cm^{-3} (a number density ~ 10 particles cm^{-3}, appropriate for an ionized region). From Equation 1 the radius of the swept-up shell will be

$$R_{MS} = 48.8\ \dot{M}_{-7}^{1/5}\ v_{2500}^{2/5}\ \rho_{10}^{-1/5}\ {t_{10}}^{3/5} \quad \text{pc} \quad (3)$$

where ρ is in units of 2.34×10^{-24} g cm^{-3}. However we note that often, especially for less massive stars whose lifetime is large, the bubble will come into pressure equilibrium with its surroundings at an early stage, and thereafter will stall. The radius of the bubble may then be up to an order of magnitude smaller than is given in Equation 3 (see Dwarkadas 2006b, 2007b).

The ratio S_m of the mass swept up by the shell to the total mass in the wind is given by:

$$S_m = \left(\frac{M_{sh}}{M_{wind}}\right) = \frac{4\pi}{3}\frac{R_{sh}^3 \rho_a}{\dot{M}t} = \frac{4\pi}{3}\ \frac{0.76^3}{2^{3/5}}\ \left(\frac{{v_w}^3 t^2 \rho}{\dot{M}}\right)^{2/5} \quad (4)$$

where ρ_a is the ambient density. For the MS this becomes

$$S_m = 1.54 \times 10^5\ v_{2500}^{6/5}\ t_{10}^{4/5}\ \rho_{10}^{2/5}\ \dot{M}_{-7}^{-2/5} \quad (5)$$

The wind velocity decreases slowly so the average velocity over the entire main sequence phase could be lower than that used. The duration of the main sequence phase also depends on the mass of the star, decreasing with increasing mass, and the mass-loss rate may vary, becoming increasingly higher as the MS phase comes to and end. Also, as noted above, in several cases the bubble will not reach this radius but may stagnate at a smaller radius. Due to all these reasons the ratio given in Equation 5 may be reduced by up to a couple of orders of magnitude. However clearly the mass swept up by the shell significantly dominates over the mass expelled in the wind, and the wind material is not significant for the dynamics. Due to the large mass of the swept-up shell compared to that of the wind, the subsequent evolution is generally contained within the main-sequence bubble. Thus, the radius of the bubble does not change significantly after the main-sequence stage, although the internal structure may undergo substantial change.

The swept-up mass lies in a thin, dense shell surrounding the bubble cavity, which consists of an inner freely expanding wind region followed by a region of almost constant density. The total wind mass ejected over time t is $\dot{M}t$. The mass in the freely expanding wind is $\dot{M}R_t/v_w$ (R_t = radius of wind termination shock). Since $v_w\ t >> R_t$ by the end of the MS phase, a lower limit to the average cavity density is obtained by assuming that the wind material is uniformly distributed:

$$\rho_{bub} = \frac{3\dot{M}t}{4\pi R_{sh}^3} = \frac{3}{4\pi\ 0.76^3}\left(\frac{2\dot{M}^{2/3}\rho_a}{v_w^2}\right)^{3/5} t^{-4/5} \quad (6)$$

which for the main sequence stage can be written as

$$\rho_{bubMS} = 1.5{\times}10^{-28}\ \dot{M}_{-7}^{2/5}\ \rho_{10}^{3/5}\ v_{2500}^{-6/5}\ {t_{10}}^{-4/5}\ \mathrm{g\ cm^{-1}} \quad (7)$$

Although this is a lower limit, especially if the bubble stalls early in the MS phase, it can be seen that the density in the interior of the bubble is on the order of $10^{-4} - 10^{-3}$ particles cm^{-3}, orders of magnitude lower than that of the surrounding medium.

The position of the wind-termination shock is of interest. An accurate calculation is provided in Weaver et al. (1977) and Chevalier & Imamura (1983). To obtain a simple approximate expression we assume that the shock is strong, the shock jump is a factor of 4, and the bubble density is approximately constant at the post-shock value. In order to accommodate the results of W77, which indicate that the density in the shocked wind increases by about a factor of 2 close to the contact discontinuity, we include a factor α, with $1 \lesssim \alpha \lesssim 2$. The total wind mass emitted over time t is $\dot{M}t$, and the mass of the freely expanding wind is $\dot{M}R_t/v_w$. The difference between the two gives the total mass of the shocked wind region between R_c and R_t, where it is assumed that $R_c \approx R_{sh}$:

$$\dot{M}t - \frac{\dot{M}R_t}{v_w} = \frac{4\pi}{3}(R_c^3 - R_t^3)\frac{4\alpha\dot{M}}{4\pi R_t^2 v_w} \quad (8)$$

which gives

$$\frac{R_t}{R_c} = \left[1 + \frac{3}{4\alpha}\left(\frac{v_w}{R_t/t} - 1\right)\right]^{-1/3} \quad (9)$$

Note that this equation is similar to Equation 13 in Chevalier & Imamura (1983), if we take $M_2 >> 1$, and assume $s_2 = R_t/t$. For our purposes this approximation is sufficient. We can simplify this further by noting that in general $v_w t/R_t >> 1$. Then we get:

$$R_t = \left[\frac{4\alpha R_c^3}{3 v_w t}\right]^{1/2} \quad (10)$$

For the parameters of the MS star, this gives

$$R_t = 2.43\ \alpha^{1/2}\ v_{2500}^{1/10}\ {t_{10}}^{2/5}\ \rho_{10}^{-3/10}\ \dot{M}_{-7}^{3/10}\ \ \mathrm{pc} \quad (11)$$

The small value of the wind termination shock shows that the hot shocked wind occupies most of the volume of the main sequence bubble.

2.2. *Post Main Sequence Phases*

Stars with M $\leq 50 M_\odot$ generally become a red supergiant (RSG) after leaving the MS. These stars have large envelopes and slow winds (10-20 km s^{-1}) with a high mass loss rate of 10^{-5} to 10^{-4} $M_\odot$ yr^{-1}. This creates a high density region around the star, confined by the pressure of the main-sequence bubble. For a RSG lifetime of about 200,000 years the total energy input in the RSG phase is

$$E_{RSG} = 8\ \times 10^{46}\ \dot{M}_{-4}\ v_{20}^2\ t_{0.2}\ \ \mathrm{ergs} \quad (12)$$

where $\dot{M}_{-4}$ is the mass loss rate in terms of $10^{-4} M_\odot$ yr^{-1}, v$_{20}$ is velocity in units of 20 km s^{-1}, and time is in units of million years, $t_{0.2} = 0.2 \times 10^6$ years.

Note that the RSG stage does not generally form a wind-blown bubble, because the velocity of the RSG wind is much lower than that of the medium (MS wind) into which it is blowing. However it does lead to a new pressure equilibrium. Since the total ram pressure of the RSG wind is different from that of the MS wind, the position of the wind termination shock will change. The new position can be found by equilibrating the ram pressure (ρv_w^2) to the thermal pressure in the MS bubble. According to W77 the thermal pressure in the MS bubble is given by

$$P_{bub} = 0.163\ L^{2/5}\ {\rho_a}^{3/5}\ t^{-4/5} \quad (13)$$

Equating to the ram pressure of the RSG wind gives the position of the wind termination shock:

$$R_{tRSG} = \left[\frac{\dot{M_{RSG}} v_{RSG}}{4\pi\ P_{bub}}\right]^{1/2} \quad (14)$$

$$= 8.85\ \dot{M}_{R-4}^{0.5}\ {v_{R20}}^{0.5}\ \dot{M_{MS}}_{-7}^{-1/5}\ {v_{MS}}_{2500}^{-2/5}\ {\rho_{10}}_a^{-3/10}\ {t_{MS}}_{10}^{2/5}\ \mathrm{pc} \quad (15)$$

where in the last expression the subscript R refers to the RSG wind and the subscript MS to the main sequence wind. It is not clear however if the RSG wind will always be able to expand out to the distance required to attain the new pressure equilibrium, and therefore in some cases the pressure equilibrium may never be attained.

The RSG wind with its low velocity expands a distance R_{RSG}, with wind density ρ_{RSG}

$$R_{RSG} = \kappa\ 4.2\ v_{20}\ t_{0.2}\ \mathrm{pc}; \quad (16)$$

$$\rho_{RSG} = 2.81 \times 10^{-23}\ \dot{M}_{-4}\ v_{20}^{-1}\ r_{pc}^{-2} \quad (17)$$

where we have added a factor $\kappa \geq 1$ to account for the fact that neither the transition, nor the change in velocity, from the MS to the RSG phase is instantaneous. Given the size of the MS bubble, it is clear that the RSG wind region will generally be confined

to a small fraction of the main-sequence bubble. The total mass lost during the RSG phase is

$$M_{RSG} = 20\ \dot{M}_{-4}\ t_{0.2}\ \ M_\odot \qquad (18)$$

Thus although total energy of the outflow in the RSG stage is small compared to the MS stage and the subsequent Wolf-Rayet stage, a large amount of stellar mass may be lost in the RSG stage.

Some stars may go from the RSG to a blue supergiant (BSG) stage, as in the case of the progenitor of SN 1987A. The bipolar structure seen around the object is often interpreted as resulting from the interaction of a BSG and RSG wind. This is discussed further in § 4. The wind parameters in this case are uncertain, but the mass-loss rate appears to be lower than even the MS stage, while the wind velocity is intermediate between the MS and RSG stage.

Solar metallicity stars above 30-35 $M_\odot$ end their lives as Wolf-Rayet (W-R) stars, although they may go through a luminous blue variable (LBV) stage. The mass-loss decreases somewhat to about $10^{-6} - 10^{-5} M_\odot$ yr^{-1}, while the wind velocity increases to 2000 km s^{-1}. For a lifetime of 100,000 years, the total energy input in the W-R phase is then

$$E_{WR} = 4 \times 10^{49}\ \dot{M}_{-5}\ v_{2000}^2\ t_{0.1}\ \text{ergs} \qquad (19)$$

Although the total mass is less, due to the high mass-loss rate and wind velocity W-R winds may posses enough momentum to push out, and possibly break up, any dense shell surrounding the star from the previous intermediate wind stage, distributing its contents throughout the surrounding medium. Generally they will have enough momentum to collide with the MS shell, sending a reflected shock back. A W-R wind termination shock will be formed where the thermal pressure of the shocked wind bubble equals the ram pressure of the freely flowing wind.

The post-MS stages may add considerable mass to the bubble without increasing the volume much. However Equations (6) and (7) imply that, even increasing the mass ($\dot{M}t$) by a factor of 30-40 results in number densities of order $10^{-3} - 10^{-2}$ cm^{-3}. Therefore the density over the bubble interior is in general low for W-R bubbles.

Multidimensional calculation (García-Segura et al. 1996; Freyer et al. 2006; Dwarkadas 2006a) reveal the presence of hydrodynamic instabilities in many stages. In one calculation of the medium around a 35 $M_\odot$ star, Dwarkadas (2006a) found that both the RSG and subsequent W-R wind (expanding into the RSG wind) were Rayleigh-Taylor unstable (Figure 1a). These instabilities tend to break-up the RSG shell and distribute its material over the entire bubble. They may lead to the formation of blobs, clumps and filaments in the WBB. Due to density fluctuations in various stages, the bubble interior becomes turbulent by the end of the simulation.

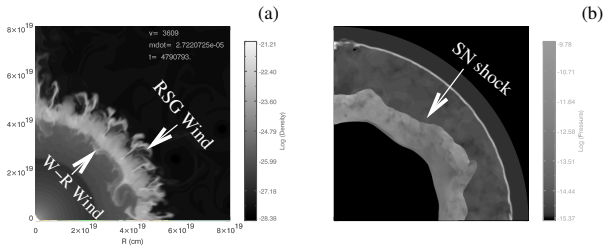

Fig. 1. (a) The evolution of the W-R wind into the RSG wind region for a 35 $M_\odot$ star. Both winds are R-T unstable. (b) The SN shock wave expanding into the density inhomogeneities in the interior can becomes wrinkled and lose its spherical shape (Dwarkadas 2006a,2007a).

Other factors will considerably modify this simple picture. Rotation of the star can lead to an increase in the mass-loss rate (Maeder & Meynet 2000). Dwarkadas & Owocki (2002) showed that a star rotating close to its break-up velocity may emit a wind preferentially in the polar direction. Mass-loss rates, which depend roughly as the square root of the metallicity, may be reduced at lower metallicities, although rotation can still lead to high rates. And the presence of a binary companion can significantly alter the evolution, as has been hypothesized for SN 1987A (Morris & Podsiadlowski 2005).

3. SUPERNOVA EVOLUTION

The above description clearly illustrates a few salient points:

• The medium around most massive stars consists of a low density cavity created in the main-sequence stage, surrounded by a dense shell.

• If the progenitor is a RSG then the density near the star may be quite high, as expected for a RSG wind density. If the RSG stage is followed by a Wolf-Rayet stage then this can distribute the RSG material over the entire WBB, and the density will be much lower.

• In either case the region close in to the star is usually a freely flowing wind, with a wind density that generally decreases as r^{-2}. However if the wind parameters change substantially with time then the density dependence may change. Several authors have suggested that the density of the medium surrounding SN 1993J decreases only as r$^{-1.5}$ (Suzuki & Nomoto 1995; Mioduszewski et al. 2001; Bartel et al. 2002).

When the star explodes as a SN the resulting shock wave will first expand in the surrounding wind medium, and then in the low density cavity. If the surrounding wind medium is a RSG then the shock wave will expand in a higher density medium, and therefore its luminosity, due to circumstellar interaction (Chevalier & Fransson 1994) will be high. If the shock wave results from the death of a W-R star then the surrounding medium density will be much lower, and the resulting luminosity will also be lower.

The shock wave will expand in the wind until it reaches the wind termination shock, after which it will continue to expand in the low density shocked-wind medium. If it was earlier expanding in a RSG wind then its luminosity will be expected to drop. If it was expanding in a Wolf-Rayet wind then the luminosity will not change much, or may in fact increase slightly as the shock wave crosses the wind termination shock.

Since most of the mass is in the dense shell, the interaction of the shock wave with the dense shell controls the relevant dynamics, which depends mainly on one parameter Λ, the ratio of the mass of the shell to that of the ejected material. Simulations for various values of Λ have been carried out by Tenorio-Tagle et al. (1990) and Dwarkadas (2005). They show that values of $\Lambda \gtrsim 1$ are dynamically important. As the value of Λ increases, the kinetic energy transmitted from the ejecta to the shell gradually increases. The collision with the shell results in a transmitted shock expanding into the shell, and a reflected shock moving back into the ejecta. It also results in an increase in the emission from the remnant, especially the optical, X-ray and radio emission. The reflected shock moves back towards the origin, thermalizing the ejecta on its way, faster than the original SN reverse shock would have. For smaller Λ the SN shock wave eventually 'forgets' about the existence of the shell, and the solution resembles what it would be in the absence of the shell. The density structure changes to reflect this. An increase in Λ results in higher velocity reflected shocks, while the transmitted shock slows down considerably. In extreme cases the transmitted shock may be trapped in the dense shell for a significant amount of time, and the shock wave may lose considerable energy to become a radiative shock wave. In such a case it can go from the free-expansion stage to the radiative stage without ever going through the Sedov or adiabatic phase. The remnant is also confined to the shell, whose size as we have seen was set in the MS stage.

The evolution of SNe in wind blown bubbles thus differs considerably from the self-similar solutions so often used to describe SN evolution in general. The radius and velocity of the remnant do not evolve in a self-similar fashion but may vary considerably once the shock expands beyond the freely-flowing wind. Furthermore the expansion parameter of the remnant δ (where $R \propto t^{\delta}$) is continuously varying, as opposed to a self-similar case where the evolution is constant. This is illustrated in Dwarkadas (2005).

In multi-dimensions (Dwarkadas 2006a,2007a) the interior of the nebula shows signs of turbulence, with significant density and pressure variations. The shock wave expanding in this medium no longer remains spherical, but becomes wrinkled due to the continuous interaction with the pressure and density inhomogeneities. It develops a corrugated structure (see Figure 1b), and its interaction with the surrounding shell no longer occurs all at once but in a piecemeal fashion, with some parts of the shock colliding with the shell before others. As mentioned before, the collision results in an increase in the luminosity. In this case the luminosity of some parts of the shell will increase first, followed by those in other parts of the shell. A similar scenario appears to be taking place in the ring around SN 1987A.

This brief description encapsulates the basic properties of the evolution of SNe in the medium around massive stars. Further details are given in Dwarkadas (2005, 2006a, 2007a). In the rest of this paper we would like to concentrate on applying the results described above to SN 1987A.

4. SN 1987A

SN 1987A provides one of the best, and most spectacular, opportunities to witness the evolution of a SN shock wave within a wind-blown bubble. The three ring structure around SN 1987A has been interpreted as an hour-glass shape bubble formed by the interaction of a blue-supergiant (BSG) and a RSG wind (Blondin & Lundqvist 1993; Sugerman et al. 2005). The relatively small size of the equatorial ring (possibly the waist of a wind-blown nebula) has ensured that we can see the shock-shell collision unfold in a short time span after the SN explosion. SN 1987A has allowed us to refine our theories of SNe evolving in the winds of massive stars, while providing confirmation of many existing ideas, and catalyzing many new ones.

Chevalier & Dwarkadas (1995) showed that the slow expansion of the radio source, its large size, and the almost linear increase in radio and X-ray emission could be understood if we assumed that the SN

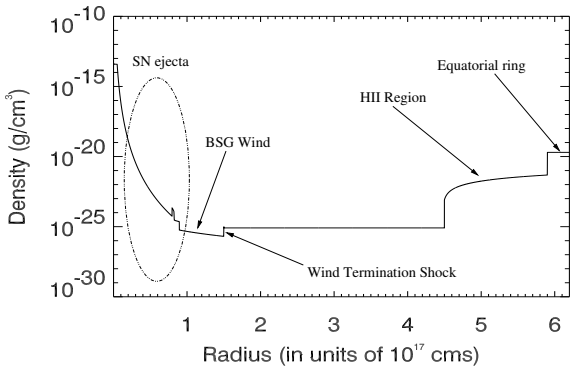

Fig. 2. The density profile just after the start of the simulation. The various regions (free expanding wind, almost constant density bubble, HII region and equatorial ring) are marked.

shock wave was interacting with an HII region inside of the inner ring. In the years since this model has been verified by Dick McCray and his collaborators (Michael et al. 1998). This model modifies the picture outlined above by including a high-density HII region inside of the outer shell, in the low density wind-driven cavity. A depiction of the surrounding medium into which the SN explodes (in the equatorial region) can be seen in Figure 2.

The morphology and dynamics of the ejecta in SN 1987A are inherently three-dimensional. The gradual appearance of bright spots around the equatorial ring (Lawrence et al. 2000), and the changes in the X-ray and optical luminosity indicate an aspherical shock interacting with several protrusions, formed perhaps by instabilities, emanating from the equatorial ring. All this presents a very complex morphology for the modeler.

Yet there are several aspects of SN 1987A that can be understood by resorting to a simple, spherically symmetric model. This includes the radius and velocity of the expanding shock wave, the reemergence of the X-ray and radio emission at around 1100 days after explosion, and the gradual increase in the X-ray emission. We present here a toy model, a spherically symmetric calculation that captures the basic idea of Chevalier & Dwarkadas (1995), and compute from this the shock dynamics, the hard X-ray emission and radio emission, which we compare with observations. The hydrodynamic simulations have been carried out using the VH-1 code, a spherically symmetric multi-dimensional finite-difference hydrodynamic code.

Figure 2 shows the initial conditions for the run. The SN ejecta, the wind termination shock of the BSG wind, the HII region and the equatorial ring are shown. The various parameters used for the run were: BSG wind mass-loss rate $\dot{M} = 5\times10^{-9}M_{\odot}$/yr, BSG wind velocity = 550 km s^{-1}, radius of wind termination shock = 1.5 $\times10^{17}$ cm, inner radius of HII region = 4.5 $\times10^{17}$ cm, inner radius of equatorial ring = 5.9 $\times10^{17}$ cm. The wind density is obtained from $\rho_w = \dot{M}/(4\pi r^2 v_w)$. The density is assumed to jump a factor of 4 at the wind termination shock, after which it remains constant up to the HII region, where the density jump is a factor of 100. The HII region density is assumed to increase steadily until the inner ring radius, whose density starts at 10^{-20} g cm^{-3} and increases linearly. The SN ejecta density varies as r^{-9}. These parameters were initially selected based on observational and theoretical work by Lundqvist (1998), Michael et al. (1998), Manchester et al. (2002), Park et al. (2006), and then modified to obtain a better fit to the observations.

In a future paper we will discuss the detailed hydrodynamics of the evolution. Herein we concentrate on the main results. The radius and velocity of the forward shock wave are shown in Figure 3. These quantities are in good agreement with 2 important observations: (1) Radio data from Manchester et al. (2002) which suggests that the shock velocity reduces abruptly from a large value (> 35000 km s^{-1}) to a value of around 3000 km s^{-1} around day 1100; and (2) X-ray observations (Park et al. 2005, 2006) which indicate that around day 6000-6200 the shock velocity decreased to about 1500-1600 km s^{-1}.

Figure 4 shows an approximate computation of the radio emission from the remnant. We follow the prescription of Chevalier (1982), assuming that the radio emitting region lies between the forward and reverse shocks, with the optically thin radio luminosity being given by

$$L_\nu \propto 4\pi R^2 \Delta R K B^{(\gamma+1)/2} \nu^{(\gamma-1)/2} \qquad (20)$$

where L_ν is the radio luminosity at frequency ν, ΔR is the thickness of the synchrotron emitting region, B is the magnetic filed, and the distribution of accelerated particles is assumed to be a power-law $N(E) = KE^{-\gamma}$. We further assume that both B and K scale simply as the hydrodynamic variables:

$$U_B = \epsilon_B U_{th}; \qquad U_{rel} = \epsilon_r U_{th} \qquad (21)$$

where U_B is the magnetic energy density, U_{rel} is the relativistic particle energy density, and U_{th} is the thermal energy density. The value of γ is taken to be 2.7 (Manchester et al. 2002).

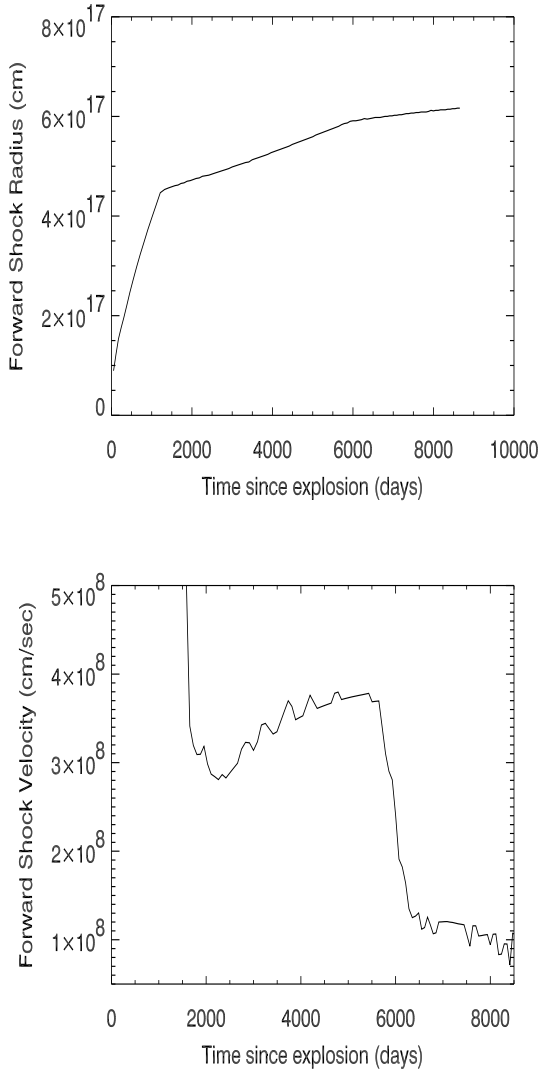

Fig. 3. The time evolution of the radius (top) and velocity (bottom) of the SN forward shock wave.

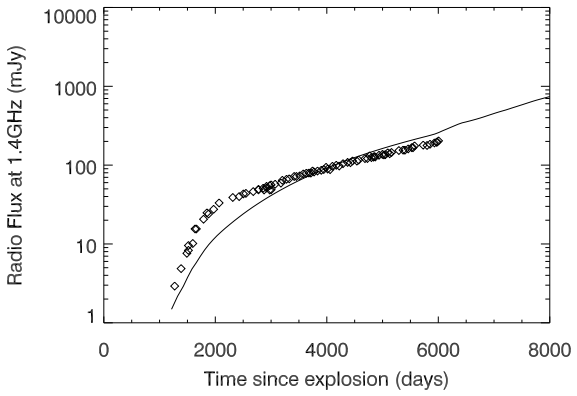

Fig. 4. The evolution of the radio luminosity with time, assuming that the parameter K is constant.

In Figure 4 the solid line shows our prediction of the radio luminosity, while the symbols represent the observed data at 1.4 GHz (Manchester et al. 2002). While the fit over the observed range is within a factor of a few, we find it difficult to get the correct linear slope. In our calculations the emission is usually increasing quadratically or faster, and by the time the shock hits the ring the radio emission begins to increase at an increasingly fast pace, which is not found in the observations. In our exploration of the parameter space we have not found a suitable set of parameters which generate a linear increase in radio luminosity.

This model is unusual in that the best fit is obtained when either the magnetic field or the parameter K representing relative particle energy density is assumed constant, with a slight preference for the latter. The reason why either quantity being constant works is due to the scaling in Equation 20. The important parameter is the quantity $KB^{(\gamma+1)/2}$. With $\gamma \sim 3$, this parameter becomes KB^2. Coupled with the scaling in Equation 21 this implies that either K constant and $B \propto P^{0.5}$, or B constant and $K \propto P$, both give $KB^2 \approx U_{th} \propto P$, where P is the thermal pressure. Thus this behavior is simply a result of γ being close to 3. It is not clear why a constant value for either quantity works best.

Figure 5 shows a comparison of the hard X-ray luminosity computed using the CHIANTI code (Dere et al. 1997; Landi et al. 2006). According to Park et al. (2005, 2006) the soft x-ray emission may be coming from the interaction of the shock wave with the protrusions in the ring. Furthermore line emission forms a strong component of the soft x-rays. These computations are beyond the scope of this paper, and we have concentrated only on the hard x-ray emission. We also assume that, for the given shock speed, the electron temperature is much lower than the ion temperature by a factor of 50 (see Ghavamian et al. 2006). This provides a reasonable fit to the X-ray emission. The solid line in Figure 5 is the emission calculated from our simulations, the data points are from Park et al. 2006. The comparison is reasonably good before the shock hits the ring, but there is a significant bump in the luminosity upon shock-ring interaction, something that is not seen in the data. Most of the hard X-ray emission appears to arise from the reverse-shocked ejecta.

There are several shortcomings to this simple spherically symmetric approach, and the subsequent computation of the radio and X-ray emission. Rel-

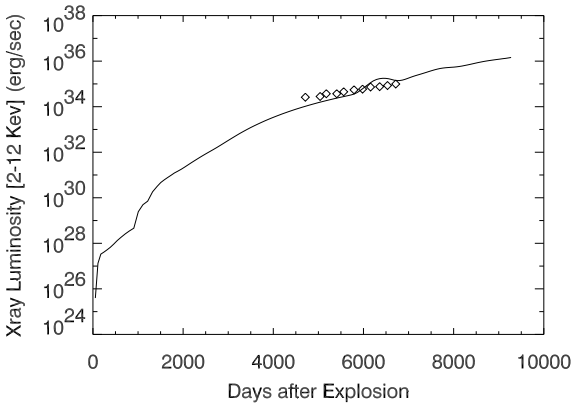

Fig. 5. The variation of the hard X-rays with time. T_e = 0.02 T_i, where 'e' = electrons and 'i' = ions. The emission is mostly coming from the reverse-shock region.

ativistic electrons may not be injected in a power-law fashion, the magnetic and/or relativistic particle energy density may not vary as the hydrodynamic variables, or the variations may be different as the shock traverses the various density structures. The spectral index varies somewhat over the evolution (Manchester et al. 2002). The expansion is not spherically symmetric, so a spherically symmetric model may not necessarily work well. There is the possibility that with aspherical expansion light travel time effects may come into play. The ratio of the electron to ion (post-shock) temperature, assumed constant here, may vary throughout the evolution. There will be contribution to the X-rays from the shock wave hitting the protrusions from the equatorial ring, which will be discussed in a more comprehensive model in future. We cannot hope to get much better agreement from such a simplified model, and it is satisfying that it does give reasonably good agreement with the observed data.

In a future paper, we will discuss in more detail the hydrodynamics of the evolution and the reverse shock dynamics, which space constraints do not permit us to include herein. We will investigate more thoroughly the emission from different regions, as well as the soft xray emission. What is also needed is a direct computation of the medium around SN 1987A, including the ionization from the star and the formation of the HII region, at least in the equatorial plane. These will be addressed in future.

VVD is supported by award # AST-0319261 from the National Science Foundation, and by NASA through grant # HST-AR-10649 awarded by the Space Science Telescope Institute. I would like to thank the organizers, and Guillermo García-Segura in particular, for an extremely broad and interesting conference, and for their gracious hospitality. Very helpful conversations with Roger Chevalier and Sangwook Park are greatly acknowledged.

REFERENCES

Bartel, N., et al. 2002, ApJ, 581 , 404
Blondin, J. M., & Lundqvist, P. 1993, ApJ, 405, 337
Chevalier, R. A. 1982, ApJ, 259, 302
Chevalier, R. A., & Dwarkadas, V. V. 1995, ApJ, 452, L45
Chevalier, R. A., & Fransson, C. 1994, ApJ, 420, 268
Chevalier, R. A., & Imamura, J. N. 1983, ApJ, 270, 554
Dere, K. P., et al. 1997, A&AS, 125, 149
Dwarkadas, V. V. 2007a, Ap&SS, 307, 153
_____. 2007b, MNRAS, in preparation
_____. 2006a, ApJ, submitted
_____. 2006b, in AAS Meeting 209, #17.25
Dwarkadas, V. V. 2005, ApJ, 630, 892
Dwarkadas, V. V., & Owocki, S. P. 2002, ApJ, 581, 1337
Freyer, T., Hensler, G., & Yorke, H. 2006, ApJ, 638, 262
García-Segura, G., Langer, N., & Mac Low,M. M. 1996, A&A, 316, 133
Ghavamian, P., Laming, J. M., & Rakowski, C. E. 2006, ApJL, 654, L69
Kudritzki, R. P., & Puls, J. 2000, ARA&A, 38, 613
Landi, E., et al. 2006, ApJS, 162, 261
Lawrence, S. S., Sugerman, B. E., Bouchet, P., Crotts, A. P., Uglesich, R., Heathcote, S. 2000, ApJ, 537, 123
Lundqvist, P. 1999, ApJ, 511, 389
Maeder, A., & Meynet, G. 2000, ARA&A, 38, 143
Manchester, R. N., et al. 2002, PASAu, 19, 207
Michael, E., McCray, R., Borkowski, K. J., Pun, C. S. J., & Sonneborn, G. 1998, ApJ, 492, L143
Mioduszewski, A. J., Dwarkadas, V. V., & Ball, L. 2001, ApJ, 562, 669
Morris, T., & Podsiadlowski, P. 2005, in ASP Conf. Ser. 342, Supernovae as Cosmological Lighthouses, ed. M. Turatto, S. Benetti, L. Zampieri, & W. Shea (San Francisco: ASP), 194
Park, S., Zhekov, S. A., & McCray, R. 2006, ApJ, 646, 1001
Park, S., Zhekov, S. A., Burrows, D. N., & McCray, R. 2005, ApJ, 634, 73
Sugerman, B., Crotts, A. P. S., Kunkel, W. E., Heathcote, S. R., & Lawrence, S. S. 2005, ApJS, 159, 60
Suzuki, T., & Nomoto, K. 1995, ApJ, 455, 658
Tenorio-Tagle, G., Bodenheimer, P., Franco, J., & Rozyczka, M. 1990, MNRAS, 244, 563
Weaver, R., McCray, R., Castor, J., Shapiro, P., & Moore, R. 1977, ApJ, 218, 377